EDGE ARTICLE

Check for updates

Equilibrating parent aminomercaptocarbene and CO_2 with 2-amino-2-thioxoacetic acid *via* heavy-atom quantum tunneling†

Bastian Bernhardt, [iD] ‡ Markus Schauermann, [iD] ‡ Ephrath Solel, [iD]
André K. Eckhardt [iD] § and Peter R. Schreiner [iD] *

The search for methods to bind CO_2 and use it synthetically as a C_1-building block under mild conditions is an ongoing endeavor of great urgency. The formation of heterocyclic carbene–carbon dioxide adducts occurs rapidly when the carbene is generated in solution in the presence of CO_2. Here we demonstrate the reversible formation of a complex of the hitherto unreported aminomercaptocarbene ($H_2N–\ddot{C}–SH$) with CO_2 isolated in solid argon by photolysis of 2-amino-2-thioxoacetic acid. Remarkably, the complex disappears in the dark as deduced by time-dependent matrix infrared measurements, and equilibrates back to the covalently bound starting material. This kinetically excluded process below *ca.* 8 K is made possible through heavy-atom quantum mechanical tunneling, as also evident from density functional theory and *ab initio* computations at the CCSD(T)/cc-pVTZ level of theory. Our results provide insight into CO_2 activation using a carbene and emphasize the role of quantum mechanical tunneling in organic processes, even involving heavy atoms.

Introduction

Incorporating CO_2 in industrial synthesis for basic chemicals, drugs, or fuels is a key goal in sustainable chemistry[1,2] and much effort has been devoted to develop CO_2 activating systems: besides frustrated Lewis pairs,[3] ionic liquids,[4] superbases,[5] poly-oxometallates,[6] and phosphorus ylides,[7] N-heterocyclic carbenes (NHCs) can be used to activate CO_2.[8,9] Such carbenes form carboxylates that can be further used for synthetic applications, *e.g.*, for carbene catalyzed carba-, sulfa-, and phospha-Michael additions[10] or as catalysts for other carbene-promoted CO_2 fixation reactions,[11–16] *e.g.*, as organic carbonates.[17] Azolium carboxylates are remarkably stable,[18] because intramolecular neutralization even through transfer of the R^3-group does not occur (Scheme 1).[19] The zwitterionic structure, however, also implies that charge separation has to occur in the attack of the carbene on the highly unreactive carbon of CO_2. NHC-carboxylates can be used as carbene-precursors when CO_2 is thermally extruded *in situ*. Some decarboxylation reactions can be achieved photochemically, *e.g.*, acetic acid extrudes CO_2 when irradiated with UV light.[20]

Institute of Organic Chemistry, Justus Liebig University, Heinrich-Buff-Ring 17, 35392 Giessen, Germany. E-mail: prs@uni-giessen.de

‡ These authors contributed equally.

§ Present address: Lehrstuhl für Organische Chemie II, Ruhr-Universität Bochum, Universitätsstraße 150, 44801 Bochum, Germany.

Photodecarboxylation has also been used for synthetic applications.[21] The photolysis of thiazol-2-carboxylic acid and imidazole-2-carboxylic acid results in the formation of carbene–CO_2 complexes, but the reverse reaction has not been reported.[22,23] For various $C(sp^3)$ carboxylates $^{13}CO_2$ exchange in solution was reported recently and carbon nucleophiles and enolates were postulated as intermediates.[24] Our results suggest the presence of carbene–CO_2 complexes in such reactions.

Here we present the preparation and reaction of a novel carbene, namely aminomercaptomethylene (**1**, $H_2N–\ddot{C}–SH$) in its complex with CO_2 (**1**-CO_2) that reacts back to 2-amino-2-
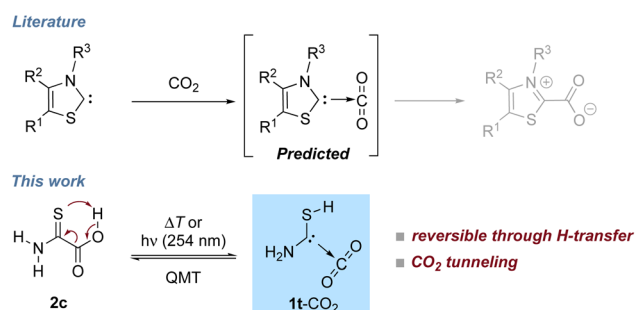
Scheme 1 In solution NHCs add to CO_2 to form carboxylate zwitterions (top, gray). In the present study **2c** photodecarboxylates to give **1t**-CO_2. This hetero-ene-type reaction is reversible under cryogenic conditions and dominated by QMT below *ca.* 8 K indicating non-covalent bound complexes as intermediates of the carboxylate formation.

thioxoacetic acid (2) under cryogenic conditions (Scheme 1). The concomitant transfer of a proton onto the CO_2 moiety leads to a neutral system instead of a zwitterion as in case of the azolium carboxylates, and this process is associated with a very low barrier.

Additionally, we demonstrate that the association reaction is accelerated through heavy-atom quantum mechanical tunneling (QMT) that opens new possibilities for affecting the reactions of CO_2 with carbenes or other nucleophiles. In this context we demonstrate the first evidence for 1, the parent structure of nature's thiazol-2-ylidene active site in, e.g., thiamine (vitamin B1) and pyruvate decarboxylase,[25] in its complex with CO_2. Coincidently, 1-CO_2 resembles a rare example of a spectroscopically characterized member of the family of mercaptocarbenes (R–C̈–SH) of which hydroxymercaptomethylene was the first spectroscopically identified member.[26] Spectrometric evidence has been reported for parent mercaptomethylene.[27,28]

Under cryogenic conditions the contribution of QMT to the overall reaction rate is larger compared to ambient conditions and sometimes completely determines the qualitative outcome of a reaction.[29–31] While proton tunneling is a rather common feature, heavy-atom QMT is encountered less frequently.[32–35] However, sometimes even larger groups are transferred as in the case of trifluoroacetyl nitrene, which reacts to trifluoromethyl isocyanate by transferring the CF_3-group in a formal [1,2]-shift via QMT.[36]

High-vacuum flash pyrolysis (HVFP) of α-keto carboxylic acids gives rise to the corresponding hydroxycarbenes that have been investigated via matrix isolation spectroscopy.[31,37–43] Besides their intriguing QMT behavior, some hydroxycarbenes add to carbonyls in nearly barrierless carbonyl–ene reactions.[44] The reaction 1t-CO_2 → 2c (Scheme 1) resembles another example of this reaction type. In analogy to these studies, we used 2 as the precursor for the generation of 1 complexed with CO_2.

Results and discussion

We synthesized 2 via saponification of commercially available ethyl thiooxamate (see the ESI and Fig. S1† for details). After deposition of 2 on a CsI window at 3 K together with a large excess of Ar, we exclusively observe its most stable anti-(E)-conformer 2c (Fig. 1). The anti-(Z)-conformer 2t is 4.3 kcal mol^{-1} higher in energy (CCSD(T)/cc-pVTZ) and, hence, not populated at 3 K. To isolate free aminomercaptomethylene 1 we performed multiple HVFP experiments exposing 2 to pyrolysis temperatures ranging from 300 up to 1150 °C. However, we could not detect even traces of 1 and only observed CO_2 and thioformamide together with small amounts of its thiolimine tautomer[45] as the pyrolysis products. This result is not completely unexpected as the corresponding carbonyl species (here a thioamide) has been the main pyrolysis product in all our previous studies on the matrix isolation of hydroxycarbenes, which follows similar strategies.[29] Furthermore, the computed Gibbs free potential energy hypersurface (PES) of the pyrolysis explains the absence of 1 in such experiments (cf. ESI,
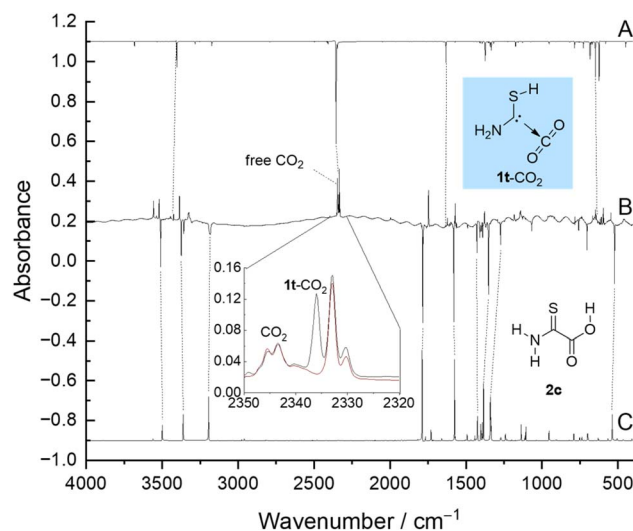

Fig. 1 Experimental matrix-IR difference spectrum (B) of spectra measured before and after 4 min of irradiation at 254 nm compared with the anharmonic spectrum of 1t-CO_2 (A) and 2c (C) computed at the B3LYP/6-311++G(3df,3pd) level of theory (anharmonic). Increasing bands not assigned here are discussed in the ESI.† (Inset) Spectra recorded before (black) and after (red) keeping the matrix in the dark for 70 h. Other time-dependent band profiles are shown in Fig. S14–S23.†

Fig. S49†). Fortunately, we were able to isolate the desired carbene 1 complexed with CO_2 photochemically as outlined in the following.

Upon UV irradiation there are several conceivable reaction paths of 2c. Photoinduced rotamerizations of carboxylic acids[46–50] and isomerizations of thioamides to thiolimines[51–62] are well known under cryogenic conditions. As 2c contains both of these functionalities, many photoproducts can be envisaged, e.g., the higher lying conformer 2t and 16 conformationally distinct thiolimines, which are 11.4 to 34.4 kcal mol^{-1} higher in energy than 2c (B3LYP/6-311++G(3df,3pd), see the ESI† for an energetic ranking (Fig. S43†) and experimental data of the rotamerization (Fig. S24†) and tautomerization (Fig. S27†) of 2). Furthermore, we observed the formation of a complex of trans-1 and CO_2 (1t-CO_2) evidenced by a characteristic matrix infrared (IR) band with maxima at 2336.1, 2333.2, and 2330.4 cm^{-1} in good agreement with the computed antisymmetric CO_2 stretching vibration at 2356.7 cm^{-1} (B3LYP/6-311++G(3df,3pd), anharmonic) in the complex. Weaker bands at 3444.9 (computed: 3404.6), 1634.8 (1633.0), and 641.8 (625.3) cm^{-1} can be assigned to 1t-CO_2 as well. These bands reach their maximum intensity after 4 min of irradiation at 254 nm (Fig. 1). The assignment is further supported by comparing experimental and computed shifts of perdeuterated 1t-CO_2-d_3 (ESI, Table S2†).

Much to our surprise, once generated, 1t-CO_2 converts back to 2c in the dark. The half-life ($t_{1/2}$) of this process depends on the matrix site[63] and can be derived by monitoring the time-dependent band profile of the antisymmetric CO_2 stretching vibration of 1t-CO_2. The decay of the maximum at 2336.1 cm^{-1} yields $t_{1/2} = 26$ min (3 K) while the maximum at 2333.2 cm^{-1}

yields $t_{1/2} = 3.8$ d (20 K, no reaction at 3 K). The third maximum (2330.4 cm^{-1}) cannot be reliably evaluated due to its small intensity and long half-life. Distinct matrix sites presumably lead to different distances between the two fragments in $1t$-CO$_2$, which result in different half-lives. The first value is in excellent agreement with CVT/SCT//B3LYP/6-311+G(d,p) computations yielding $t_{1/2} = 55$ min at 3 K for the $1t$-CO$_2 \rightarrow 2c$ reaction while the second value agrees well with CVT/SCT//B3LYP/6-311++G(3df,3pd) computations ($t_{1/2} = 7.6$ d). The C–C distance in $1t$-CO$_2$ is 2.971 Å at the first and 3.005 Å at the latter level of theory; the activation barriers towards $2c$ are reduced to 1.9 and 2.2 kcal mol^{-1}, respectively. For details on the kinetic analyses see the ESI.†

Even though the computed barrier of 4.2 kcal mol^{-1} (CCSD(T)/cc-pVTZ) is low, the $1t$-CO$_2 \rightarrow 2c$ reaction cannot occur thermally at 3 K, and only QMT explains the experimental observation. To ensure that there is no activation by the spectrometer's light source we repeated the experiment measuring every 5 min while the matrix was not exposed to the spectrometer globar beam between measurements. We also prepared perdeuterated $1t$-CO$_2$-d_3 whose half-life extends to $t_{1/2} = 36$ min (3 K) in the first and $t_{1/2} = 5.1$ d (20 K) in the second matrix site (see the ESI† for details). This is in good agreement with CVT/SCT//B3LYP/6-311++G(3df,3pd) computations ($t_{1/2} = 259$ min at 3 K, second matrix site: 7.6 d at 20 K). This effect is small (KIE = 1.4 at 3 K, computed: 4.7 at 3 K) owing to the minute movements of the H/D atoms in the QMT process (*vide infra*). Additionally, we performed kinetic measurements at temperatures between 3 K and 12 K to solidify the QMT mechanism of the reaction $1t$-CO$_2$ (2336.1 cm^{-1}) $\rightarrow 2c$ (Fig. 2). Note that at 20 K we could not detect $1t$-CO$_2$ in this matrix site presumably due to its very fast reaction ($t_{1/2} < 1$ min).
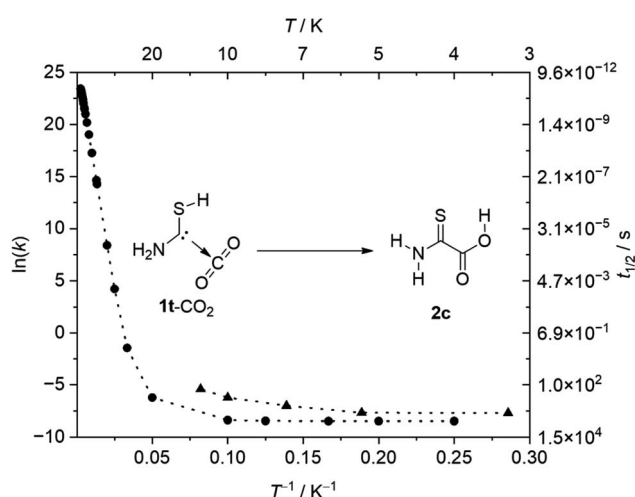
The logarithmic rate *vs.* inverse temperature plots (Arrhenius plots) of theory and experiment in Fig. 2 agree well with the regions of Arrhenius and non-Arrhenius behavior, underlining our QMT hypothesis. We conclude that at temperatures below *ca.* 8 K QMT dominates this reaction entirely. Above *ca.* 20 K the rate grows exponentially since the barrier of 4.2 kcal mol^{-1} (CCSD(T)/cc-pVTZ) can be overcome thermally. This system allows for measuring of the kinetics up to temperatures that are in the transition range between the QMT-dominated and the thermally-dominated regions.

Our result can be rationalized comparing the geometry of $1t$-CO$_2$ with that of **TS_CO$_2$** (point B; Fig. 3). In **TS_CO$_2$** the S–H bond does not elongate; the distance the hydrogen atom moves is the result of the H–S–C angle decreasing. Instead, the main movement in **TS_CO$_2$** is the two carbon atoms approaching each other by about 0.7 Å. Two hydrogen bonds form between the thiol- and the amino-group facilitating the bonding and activation of CO$_2$. Upon C–C-bond formation the curve flattens and reaches point C (Fig. 3B) corresponding to a zwitterionic structure similar to the carboxylate products in reactions of NHCs with CO$_2$ (*cf.* Scheme 1). However, point C is not a minimum on the PES ($v_i = 164.5$ cm^{-1}, B3LYP/6-311++G(3df,3pd)) and a hydrogen shift immediately occurs yielding an uncharged species. The potential of this hydrogen transfer is steep and this step does not contribute to the observable kinetics of the reaction. Hence, the measured kinetics (Fig. 2) are due to the two fragments **1** and CO$_2$ approaching each other and not the subsequent hydrogen transfer. Therefore, below *ca.* 8 K the reaction mechanism can be best described as heavy-atom QMT.

Carbene **1** possesses a singlet ground state and the vertical (adiabatic) singlet/triplet energy separation amounts to 59.4 (38.1) kcal mol^{-1} at the B3LYP/6-311++G(3df,3pd) level of
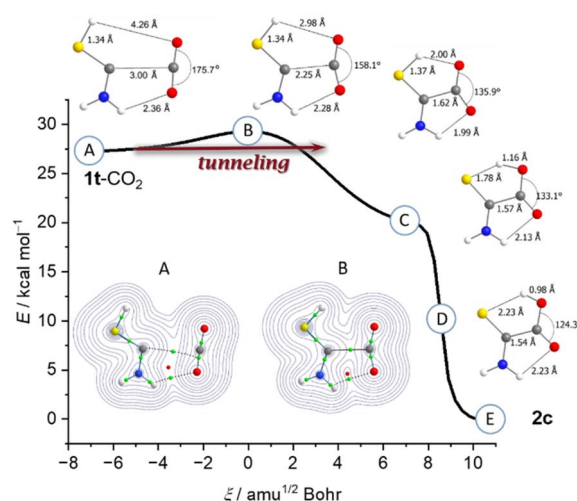

Fig. 2 Arrhenius plot of the experimental rate constants (k) of the reaction of $1t$-CO$_2$ (2336.1 cm^{-1}) to $2c$ at different temperatures (T; triangles) compared to computed rates (CVT/SCT//B3LYP/6-311+G(d,p); circles). Above *ca.* 20 K the classic thermal reactivity dominates this reaction (linear curve). Below *ca.* 8 K (constant values) this reaction can only occur *via* QMT.

Fig. 3 Intrinsic reaction coordinate (B3LYP/6-311++G(3df,3pd)) of the reaction of $1t$-CO$_2$ to $2c$. Bond critical points (green) and a ring critical point (red) in $1t$-CO$_2$ indicate bonding interactions between the carbon atoms and between oxygen and the amino group. This is also visualized by the Laplacian (inset). Once the C–C-bond formed, the H-shift occurs without further activation.

theory. In **1t**-CO_2 these values are 61.8 (57.2) kcal mol^{-1}. Complex **1t**-CO_2 is stabilized by 4.2 kcal mol^{-1} (CCSD(T)/cc-pVTZ) compared to the free fragments. A bond critical point analysis (Fig. 3, inset) of **1t**-CO_2 suggests hydrogen bonding interactions (green) between the amino group and CO_2 as well as an onset of interactions between the carbon atoms, even at a distance of nearly 3 Å. This leads to a circular arrangement of bonding interactions indicated by a ring critical point (red). The attractive interaction can be interpreted by electron donation from the carbene lone pair to the π^*-CO_2 orbital (Fig. S38†).

Complexes of carbenes with CO_2 might represent transient intermediates in carbene mediated CO_2 activation in general. We theoretically found complexes of aminomethylene,[64] dihydroxymethylene,[38] and aminohydroxymethylene[65] with CO_2 to be minimum structures on their PES. The carbonyl–ene reactions of aminomethylene and dihydroxymethylene are barrierless while the CO_2 addition of aminohydroxymethylene is associated with an activation barrier of 3.9 kcal mol^{-1} (CCSD(T)/cc-pVTZ). However, these complexes have not been observed experimentally since the mentioned carbenes have been generated under HVFP conditions in the gas phase, when entropy precludes their formation.

As noted above, a CO_2 complex of thiazolylidene has been spectroscopically identified earlier, but the back reaction, *i.e.*, CO_2 activation has not been reported. We reproduced these results and also found no evidence for the reverse reaction to take place even upon annealing the matrix to 32 K. Note that in thiazolylidene the proton has to be transferred from the NH group (and not from the SH moiety as in **1t**-CO_2). This possibility is in principle also given in **1t**-CO_2 *via* **TS15** (Fig. 4).

While the H-transfer from SH is barrierless (Fig. 4, blue), in both cases transfers from NH feature a second barrier after the formation of the zwitterion (**2*** and **13***). In the case of thiazolylidene the formation of the zwitterion itself is even

endothermic. This leads to a large barrier integral and QMT cannot take place. Accordingly, only for the reaction of **1t**-CO_2 to **2c** tunneling was observed.

Conclusions

We isolated a complex of aminomercaptomethylene with CO_2 in solid argon by photolysis of 2-amino-2-thioxoacetic acid. The carbene itself is a rare example of spectroscopically examined aminocarbenes as well as mercaptocarbenes. Once generated, the complex reacts back to the precursor in a heavy-atom quantum tunneling process at 3 K.

While NHCs readily react with CO_2 in solution to form stable carboxylates, this is not possible in the gas phase or in inert gas matrices due to the charge separation. In **1t**-CO_2 the thiol group facilitates the formation of a covalent bond by avoiding charge separation through an H shift. This, together with the heavy-atom tunneling uncovered here, opens new avenues for reactions for the activation of small molecules, in particular, CO_2.

A related mechanism, albeit thus far not considered may also operate in the initial steps of the conversion of CO_2 to formic acid, catalyzed by 1,2,3-triazole.[66]

Data availability

All experimental and computed data are collected in the ESI.†

Author contributions

B. B. and M. S. performed the matrix isolation experiments and evaluated the experimental data. B. B., M. S., E. S., and A. K. E. conducted the computational work. P. R. S. supervised the project. All authors interpreted the results and contributed to the final version of the manuscript.

Conflicts of interest

There are no conflicts to declare.

Acknowledgements

Fig. 4 IRC curves for the H-transfer in **1t**-CO_2 from the SH group and the NH_2 group (blue) compared to the reaction profile of **13** (red). All IRC curves computed at B3LYP/6-311++G(3df,3pd).

Notes and references

1 *Carbon Dioxide as Chemical Feedstock*, ed. M. Aresta, Wiley-VCH, Weinheim, 2010.

2 A. Gulzar, A. Gulzar, M. B. Ansari, F. He, S. Gai and P. Yang, *Chem. Eng. J.*, 2020, 100013.

3 C. M. Momming, E. Otten, G. Kehr, R. Frohlich, S. Grimme, D. W. Stephan and G. Erker, *Angew. Chem., Int. Ed.*, 2009, **48**, 6643.
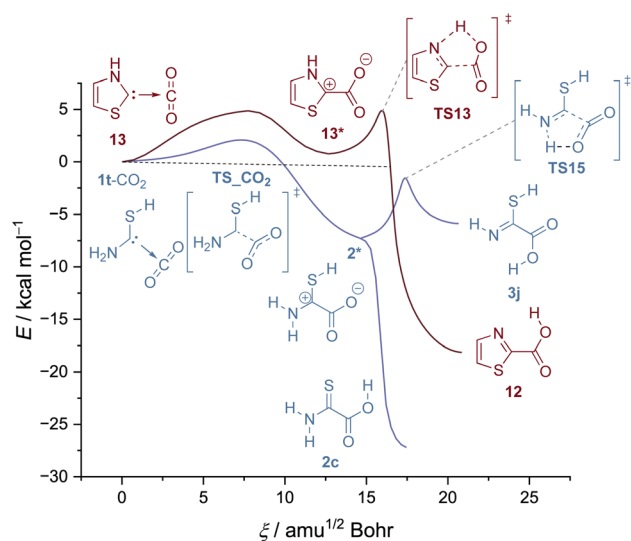
4 C. Wang, H. Luo, D. E. Jiang, H. Li and S. Dai, *Angew. Chem., Int. Ed.*, 2010, **49**, 5978.

5 C. Villiers, J. P. Dognon, R. Pollet, P. Thuery and M. Ephritikhine, *Angew. Chem., Int. Ed.*, 2010, **49**, 3465.

6 M.-Y. Wang, Q.-W. Song, R. Ma, J.-N. Xie and L.-N. He, *Green Chem.*, 2016, **18**, 282.

7 H. Zhou, G.-X. Wang, W.-Z. Zhang and X.-B. Lu, *ACS Catal.*, 2015, **5**, 6773.

8 L. Yang and H. Wang, *ChemSusChem*, 2014, **7**, 962.

9 A. Tudose, A. Demonceau and L. Delaude, *J. Organomet. Chem.*, 2006, **691**, 5356.

10 M. Hans, L. Delaude, J. Rodriguez and Y. Coquerel, *J. Org. Chem.*, 2014, **79**, 2758.

11 L. Gu and Y. Zhang, *J. Am. Chem. Soc.*, 2010, **132**, 914.

12 J. D. Holbrey, W. M. Reichert, I. Tkatchenko, E. Bouajila, O. Walter, I. Tommasi and R. D. Rogers, *Chem. Commun.*, 2003, 28.

13 H. A. Duong, T. N. Tekavec, A. M. Arif and J. Louie, *Chem. Commun.*, 2004, **40**, 112.

14 I. Tommasi and F. Sorrentino, *Tetrahedron Lett.*, 2006, **47**, 6453.

15 I. Tommasi and F. Sorrentino, *Tetrahedron Lett.*, 2005, **46**, 2141.

16 H. Zhou, W.-Z. Zhang, C.-H. Liu, J.-P. Qu and X.-B. Lu, *J. Org. Chem.*, 2008, **73**, 8039.

17 Y. Kayaki, M. Yamamoto and T. Ikariya, *Angew. Chem., Int. Ed.*, 2009, **121**, 4258.

18 D. M. Denning and D. E. Falvey, *J. Org. Chem.*, 2014, **79**, 4293.

19 L. Delaude, *Adv. Synth. Catal.*, 2020, **362**, 3259.

20 L. Farkas and O. H. Wansbrough-Jones, *Z. Phys. Chem B*, 1932, **18**, 124.

21 M. K. R. Noyori, M. Kawanisi and H. Nozaki, *Tetrahedron*, 1969, **25**, 1125.

22 G. Maier and J. Endres, *Eur. J. Org. Chem.*, 1998, **1998**, 1517.

23 G. Maier, J. Endres and H. P. Reisenauer, *Angew. Chem., Int. Ed.*, 1997, **36**, 1709.

24 P. J. M. D. Kong, E. K. J. Lui, O. Bsharat and R. J. Lundgren, *Science*, 2020, **369**, 557.

25 R. Breslow, *J. Am. Chem. Soc.*, 1958, **80**, 3719.

26 M. Schauermann and P. R. Schreiner, *J. Phys. Chem. Lett.*, 2022, **13**, 3138.

27 E. E. Gard, M. J. Kleeman, D. S. Gross, L. S. Hughes, J. O. Allen, B. D. Morrical, D. P. Fergenson, T. Dienes, M. E. Gälli and R. J. Johnson, *Science*, 1998, **279**, 1184.

28 S. Doddipatla, C. He, R. I. Kaiser, Y. Luo, R. Sun, G. R. Galimova, A. M. Mebel and T. J. Millar, *Proc. Natl. Acad. Sci.*, 2020, **117**, 22712.

29 P. R. Schreiner, *J. Am. Chem. Soc.*, 2017, **139**, 15276.

30 P. R. Schreiner, *Trends Chem.*, 2020, **2**, 980.

31 P. R. Schreiner, H. P. Reisenauer, D. Ley, D. Gerbig, C.-H. Wu and W. D. Allen, *Science*, 2011, **332**, 1300.

32 W. T. Borden, *Wiley Interdiscip. Rev.: Comput. Mol. Sci.*, 2016, **6**, 20.

33 R. S. Sheridan, in *Review Reactive Intermediate Chemistry*, 2007, p. 415.

34 C. Castro and W. L. Karney, *Angew. Chem., Int. Ed.*, 2020, **59**, 8355.

35 C. M. Nunes, A. K. Eckhardt, I. Reva, R. Fausto and P. R. Schreiner, *J. Am. Chem. Soc.*, 2019, **141**, 14340.

36 Z. Wu, R. Feng, H. Li, J. Xu, G. Deng, M. Abe, D. Bégué, K. Liu and X. Zeng, *Angew. Chem., Int. Ed.*, 2017, **129**, 15878.

37 P. R. Schreiner, H. P. Reisenauer, F. C. Pickard IV, A. C. Simmonett, W. D. Allen, E. Mátyus and A. G. Császár, *Nature*, 2008, **453**, 906.

38 P. R. Schreiner and H. P. Reisenauer, *Angew. Chem., Int. Ed.*, 2008, **47**, 7071.

39 D. Ley, D. Gerbig, J. P. Wagner, H. P. Reisenauer and P. R. Schreiner, *J. Am. Chem. Soc.*, 2011, **133**, 13614.

40 D. Ley, D. Gerbig and P. R. Schreiner, *Chem. Sci.*, 2013, **4**, 677.

41 A. Mardyukov, H. Quanz and P. R. Schreiner, *Nat. Chem.*, 2017, **9**, 71.

42 A. K. Eckhardt, F. R. Erb and P. R. Schreiner, *Chem. Sci.*, 2019, **10**, 802.

43 D. Gerbig, H. P. Reisenauer, C.-H. Wu, D. Ley, W. D. Allen and P. R. Schreiner, *J. Am. Chem. Soc.*, 2010, **132**, 7273.

44 A. K. Eckhardt, M. M. Linden, R. C. Wende, B. Bernhardt and P. R. Schreiner, *Nat. Chem.*, 2018, **10**, 1141.

45 B. Bernhardt, F. Dressler, A. K. Eckhardt, J. Becker and P. R. Schreiner, *Chem.–Eur. J.*, 2021, **27**, 6732.

46 M. Pettersson, E. M. S. Maçôas, L. Khriachtchev, J. Lundell, R. Fausto and M. Räsänen, *J. Chem. Phys. A*, 2002, **117**, 9095.

47 G. Maier, J. Endres and H. P. Reisenauer, *J. Mol. Struct.*, 2012, **1025**, 2.

48 D. Gerbig and P. R. Schreiner, *J. Chem. Phys. B*, 2015, **119**, 693.

49 M. Tsuge and L. Khriachtchev, *J. Phys. Chem. A*, 2015, **119**, 2628.

50 P. R. Schreiner, J. P. Wagner, H. P. Reisenauer, D. Gerbig, D. Ley, J. Sarka, A. G. Császár, A. Vaughn and W. D. Allen, *J. Am. Chem. Soc.*, 2015, **137**, 7828.

51 H. Rostkowska, L. Lapinski and M. J. Nowak, *Phys. Chem. Chem. Phys.*, 2018, **20**, 13994.

52 H. Rostkowska, L. Lapinski and M. J. Nowak, *J. Phys. Chem. A*, 2017, **121**, 6932.

53 S. Góbi, I. Reva, I. P. Csonka, M. C. Nunes, G. Tarczay and R. Fausto, *Phys. Chem. Chem. Phys.*, 2019, **21**, 24935.

54 S. Góbi, C. M. Nunes, I. Reva, G. Tarczay and R. Fausto, *Phys. Chem. Chem. Phys.*, 2019, **21**, 17063.

55 E. M. Brás and R. Fausto, *J. Photochem. Photobiol., A*, 2018, **357**, 185.

56 E. M. Brás and R. Fausto, *J. Mol. Struct.*, 2018, **1172**, 42.

57 D. Prusinowska, L. Lapinski, M. J. Nowak and L. Adamowicz, *Spectrochim. Acta A*, 1995, **51**, 1809.

58 M. J. Nowak, L. Lapinski, H. Rostkowska, A. Les and L. Adamowicz, *J. Phys. Chem.*, 1990, **94**, 7406.

59 M. J. Nowak, L. Lapinski, J. Fulara, A. Les and L. Adamowicz, *J. Phys. Chem.*, 1991, **95**, 2404.

60 L. Lapinski, H. Rostkowska, A. Khvorostov, M. Yaman, R. Fausto and M. J. Nowak, *J. Chem. Phys. A*, 2004, **108**, 5551.

61 L. Lapinski, H. Rostkowska, A. Khvorostov and M. J. Nowak, *Phys. Chem. Chem. Phys.*, 2003, **5**, 1524.

62 H. Rostkowska, L. Lapinski, A. Khvorostov and M. J. Novak, *J. Phys. Chem. A*, 2003, **107**, 6373.

63 T. Schleif, J. Tatchen, J. F. Rowen, F. Beyer, E. Sanchez-Garcia and W. Sander, *Chem.–Eur. J.*, 2020, **26**, 10452.

64 A. K. Eckhardt and P. R. Schreiner, *Angew. Chem., Int. Ed.*, 2018, **57**, 5248.

65 B. Bernhardt, M. Ruth, H. P. Reisenauer and P. R. Schreiner, *J. Phys. Chem. A*, 2021, **125**, 7023.

66 X. Song, Y. Meng and R. N. Zare, *J. Am. Chem. Soc.*, 2022, **144**, 16744.